



Communication

Damage in carbon fiber-reinforced concrete, monitored by electrical resistance measurement

Dragos-Marian Bontea, D.D.L. Chung*, G.C. Lee

Composite Materials Research Laboratory, Department of Mechanical and Aerospace Engineering, State University of New York at Buffalo, Buffalo, NY 14260-4400, USA

Received 17 November 1999; accepted 28 December 1999

Abstract

Damage of carbon fiber-reinforced concrete was revealed by an increase in the DC electrical resistance in the stress direction during dynamic compression. Minor damage that did not involve a change in modulus resulted in a partially reversible increase in resistance during loading at a stress above that in prior loading. Major damage that involved a decrease in modulus resulted in resistance increase occurring in every loading cycle irrespective of prior loading and in an irreversible increase in the baseline resistance. © 2000 Elsevier Science Ltd. All rights reserved.

Keywords: Microcracking; Electrical properties; Strain effect; Concrete; Carbon fibers

1. Introduction

Damage monitoring (or structural health monitoring) of a structure is valuable for hazard mitigation, whether the damage is due to use, earthquake, wind, or ocean waves. Major damage in concrete, usually accompanied by visible cracks, is obviously hazardous and can be detected by visual inspection, liquid penetrant inspection, ultrasonic inspection, and other techniques. However, minor damage that is not accompanied by visible cracks is also hazardous, as it is associated with degradation of the structural properties. Nondestructive detection of minor damage is much more challenging than that of major damage. Damage detection by flexibility change detection (i.e., detection of the change in the dynamic mechanical characteristics) is nondestructive [1], though the vibration accompanying the detection may cause minor damage. This paper addresses the monitoring of both major and minor damage, using electrical resistance measurement, which is totally nondestructive.

In short fiber-reinforced concrete, the bridging of the cracks by fibers limits the crack height to values much

smaller than those of concrete without fiber reinforcement. For example, the crack height is less than 1 μm in carbon fiber-reinforced mortar after compression to 70% of the compressive strength, but is about 100 μm in mortar without fibers after compression to 70% of the corresponding compressive strength (Fig. 9 of Ref. [2]). As a result, the regime of minor damage is more dominant when fibers are present.

Cement-reinforced with short carbon fibers is attractive due to its high flexural strength and toughness and low drying shrinkage, in addition to its strain sensing ability [3–14]. The strain sensing ability stems from the effect of strain on the microcrack height and the consequent slight pull-out or push-in of the fiber that bridges the crack [2]. Fiber pull-out occurs during tensile strain and causes an increase in the contact electrical resistivity at the fiber–matrix interface, thereby increasing the volume resistivity of the composite. Fiber push-in occurs during compressive strain and causes a decrease in the volume resistivity of the composite [2].

While reversible changes in electrical resistance upon dynamic loading relates to dynamic strain, irreversible changes in resistance relate to damage. It has been reported that the resistance of carbon fiber-reinforced cement mortar decreases irreversibly during the early stage of fatigue (the first 10% or less of the fatigue life) due to matrix damage resulting from multiple cycles of fiber pull-out and push-in

* Corresponding author. Tel.: +1-716-645-2593 ext. 2243; fax: +1-716-645-3875.

E-mail address: ddlchung@acsu.buffalo.edu (D.D.L. Chung).

[6]. The matrix damage enhances the chance of adjacent fibers to touch one another, thereby decreasing the resistivity. Beyond the early stage of fatigue and up to the end of the fatigue life, there is no irreversible resistance change, other than the abrupt resistance increase at fracture [6]. The absence of an irreversible change before fracture indicates that the mortar is not a good sensor of its fatigue damage.

Fatigue damage is to be distinguished from damage under increasing stresses. The former typically involves

stress cycling at a low and fixed stress amplitude [6], whereas the latter typically involves higher stresses. The former tends to occur more gradually than the latter. Thus, the failure to sense fatigue damage [6] does not suggest failure to sense damage in general.

In this work, the sensing of damage under increasing stresses was demonstrated in carbon fiber-reinforced concrete. The damage was found to be accompanied by a partially reversible increase in the electrical resistivity of

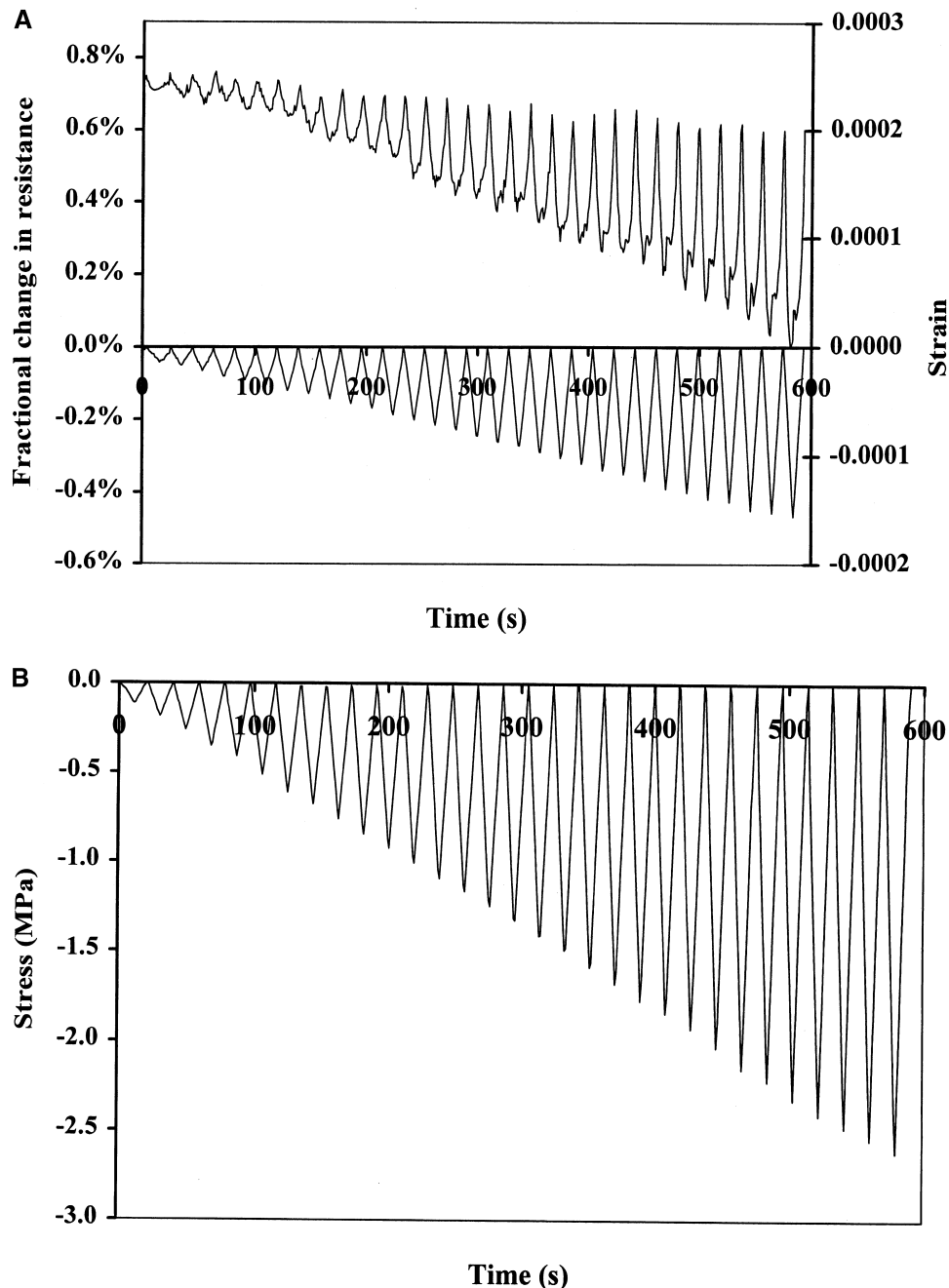


Fig. 1. Fractional change in resistance, strain (a) and stress (b) during repeated compressive loading at increasing stress amplitudes up to 20% of the compressive strength.

the concrete. The greater the damage, the larger was the resistivity increase. As fiber breakage would have resulted in an irreversible resistivity increase, the damage is probably not due to fiber breakage, but due to partially reversible interface degradation. The interface could be that between fiber and matrix. Damage was observed within the elastic regime, even in the absence of a change in modulus.

Carbon fiber-reinforced concrete can monitor both strain and damage simultaneously through electrical resistance measurement. The resistance decreases upon compressive strain and increases upon damage. This means that the

strain/stress condition (during dynamic loading) under which damage occurs can be obtained, thus facilitating damage origin identification.

Concrete differs from mortar in that it contains a coarse aggregate. Moreover, concrete is a much more common structural material than mortar. Previous work on fatigue monitoring was done on mortar only [6]. Therefore, this work is focused on damage monitoring of concrete although similar results were obtained in this work for mortar.

The objectives of this work are to investigate the ability of carbon fiber-reinforced concrete to monitor its own

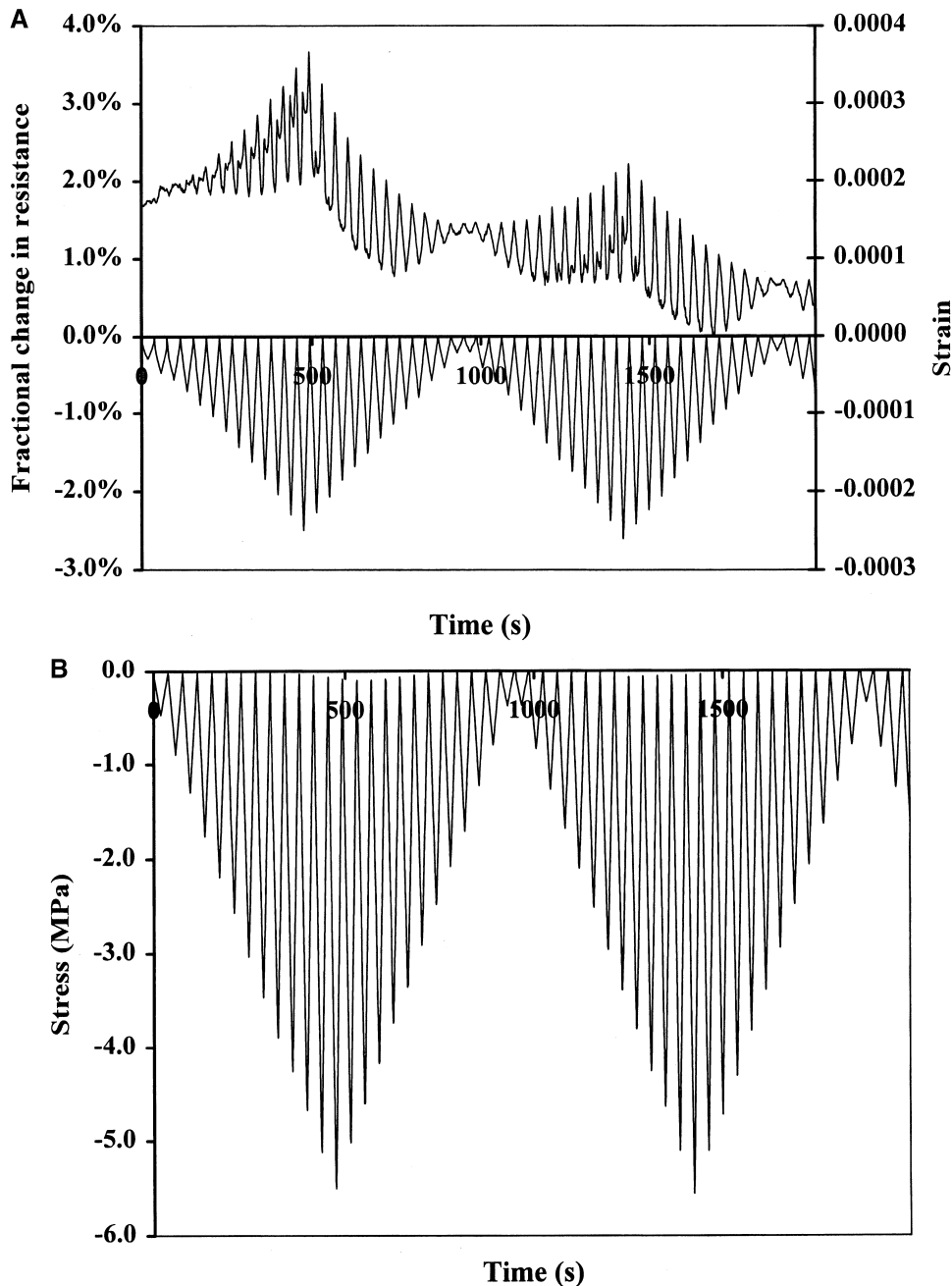


Fig. 2. Fractional change in resistance, strain (a) and stress (b) during repeated compressive loading at increasing and decreasing stress amplitudes, the highest of which was 40% of the compressive strength.

damage and to study the reversibility and stress/strain conditions of damage in carbon fiber-reinforced concrete.

2. Experimental methods

The carbon fibers were isotropic pitch-based and un-sized, as obtained from Ashland Petroleum (Ashland, KY). The fiber diameter was 15 μm . The nominal fiber length was 5 mm. Fibers in the amount of 0.5%, 1%, and 2% by weight of cement (i.e., 0.045%, 0.09%, and 0.18% by volume of composite, respectively) were used. The cement used was Portland cement (Type I) from Lafarge (Southfield, MI). Silica fume and methylcellulose were used to help the fiber dispersion [7]. The silica fume (Elkem Materials, Pittsburgh, PA, microsilica EMS 965) was used in the amount of 15% by weight of cement. The methylcellulose, used in the amount of 0.4% by weight of cement, was Methocel A15-LV from Dow Chemical, Midland, MI. The defoamer (Colloids, Marietta, GA, 1010) used whenever methylcellulose was used was in the amount of 0.13 vol.%.

Both fine and coarse aggregates were used. The fine aggregate was natural sand (99.9% SiO_2), 100% of which passed #8 US sieve. The coarse aggregate was a natural round stone, 100% of which passed #4 US sieve. The ratio of cement to fine aggregate to coarse aggregate was 1:1.5:2.5.

The water–cement ratio was 0.50. A water-reducing agent (TAMOL SN, Rohm & Hass, Philadelphia, PA; sodium salt of a condensed naphthalenesulphonic acid) was used in the amount 2% of the cement weight.

All ingredients except the coarse aggregate were mixed in a Hobart mixer with a flat beater at a high speed for 5

min. Then this mixture and the coarse aggregate were mixed in a concrete mixer at a low speed for 3 min. After this, the concrete mix was poured into oiled molds to form cubes of size 51 \times 51 \times 51 mm (2 \times 2 \times 2 in.) and cylinders of diameter 102 mm (4 in.) and height 203 mm (8 in.) for compressive testing. After pouring, an internal vibrator was used to facilitate compaction and decrease the amount of air bubbles. The samples were demolded after 24 h and then cured in a moist room (relative humidity = 100%) for 28 days.

Compressive testing was performed on a side of each cubic specimen and on the flat surface of each cylindrical specimen. The strain was measured by using a strain gage attached to the middle of a side of a specimen. The strain gage was parallel to the stress axis. Compressive testing under load control was performed using a hydraulic mechanical testing system (MTS Model 810). Testing was conducted under repeated loading at various stress amplitudes.

During compressive testing, DC electrical resistance measurement was made in the stress axis, using the four-probe method, in which silver paint in conjunction with copper wires served as electrical contacts [2]. Four contacts were around the whole perimeter of the specimen at four planes that were all perpendicular to the stress axis and that were symmetrically positioned with respect to the mid-point along the height of the specimen (i.e., two contacts were at planes above the mid-point and two contacts were at planes below the mid-point). The outer two contacts (38 mm apart) were for passing current. The inner two contacts (13 mm apart) were for measuring the voltage. A Keithley 2001 multimeter was used. Due to the small strains involved, the fractional change in resistance was essentially equal to the fractional change in resistivity.

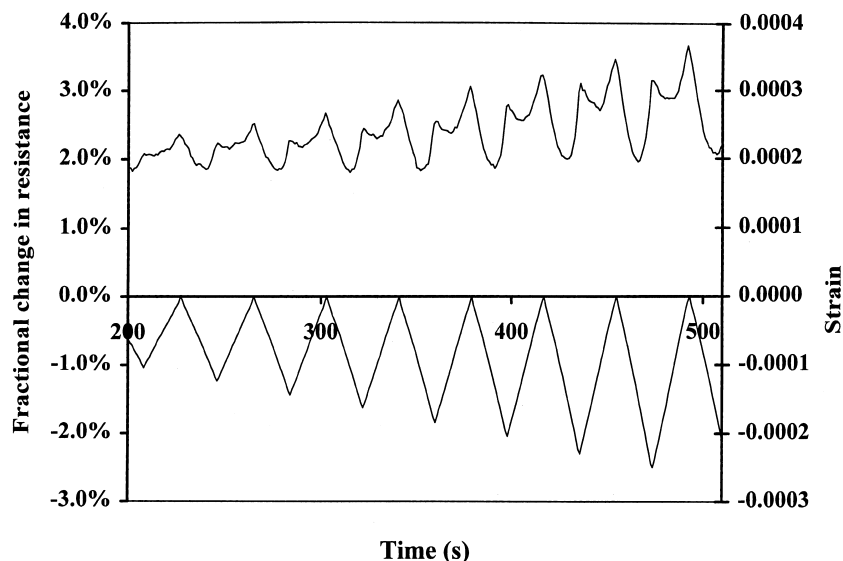


Fig. 3. A magnified view of the first 500 s of Fig. 2(a).

3. Results

Qualitatively similar results were obtained on the cubic and cylindrical specimens. Only results for the cubic specimens are shown below, because the large diameter of the cylinder did not allow the current to penetrate through the entire cross-section of the cylinder.

Qualitatively similar results were obtained for fiber contents of 2% and 1% by weight of cement, but the data were more noisy at the lower fiber content. At a fiber content of 0.5% by weight of cement, the data were too noisy to be meaningful. Therefore, only results for a fiber content of 2% by weight of cement are shown below.

At least four specimens of each type were tested. The results reported here in terms of the response of the

electrical resistance to strain and damage were consistently observed in all the specimens.

Fig. 1 shows the fractional change in resistance, strain and stress during repeated compressive loading at increasing stress amplitudes up to 20% of the compressive strength (within the elastic regime). The strain returned to zero at the end of each loading cycle. The resistance decreased reversibly upon loading in each cycle. The higher the stress amplitude, the greater was the extent of resistance decrease. As load cycling progressed, the resistance at zero load decreased gradually cycle by cycle. In addition, an extra peak in the resistance curve appeared after the first 16 cycles in Fig. 1 and became larger and larger as cycling progressed. The maximum of the extra peak occurred at the maximum stress of the cycle.

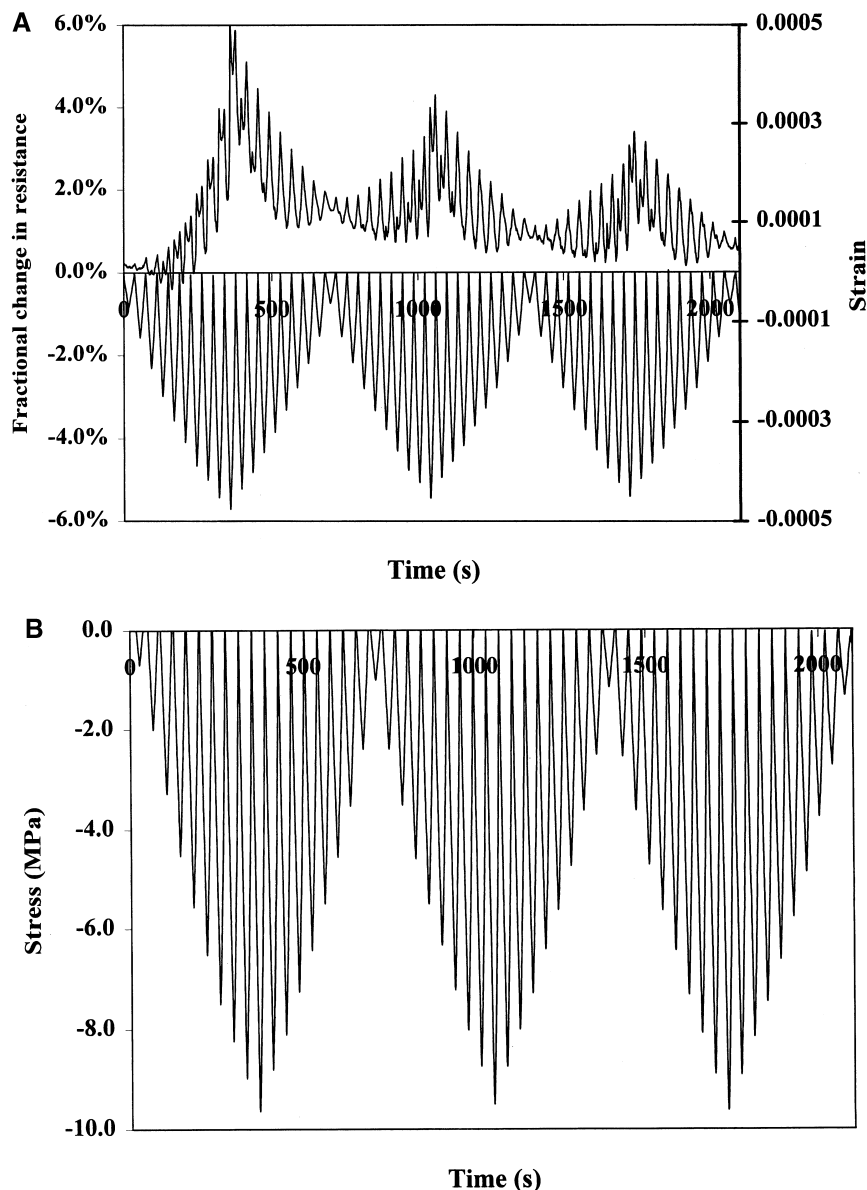


Fig. 4. Fractional change in resistance, strain (a) and stress (b) during repeated compressive loading at increasing and decreasing stress amplitudes, the highest of which was 60% of the compressive strength.

Fig. 2 shows the fractional change in resistance, strain and stress during repeated compressive loading at increasing and decreasing stress amplitudes. The highest stress amplitude was 40% of the compressive strength. A group of cycles in which the stress amplitude increased cycle by cycle and then decreased cycle by cycle back to the initial low-stress amplitude is hereby referred to as a group. Fig. 2 shows the results for two groups, plus the beginning of the third group. The strain returned to zero at the end of each cycle for any of the stress amplitudes, indicating elastic

behavior. Fig. 3 shows a magnified view of the first half of the first group. The resistance decreased upon loading in each cycle, as in Fig. 1. The extra peak at the maximum stress of a cycle grew as the stress amplitude increased, as in Fig. 1. However, in contrast to Fig. 1, the extra peak quickly became quite large, due to the higher maximum stress amplitude in Fig. 2 than in Fig. 1. In Fig. 2, there are two peaks per cycle. The original peak (larger peak) occurred at zero stress, while the extra peak (smaller peak) occurred at the maximum stress. Hence, during loading from zero stress

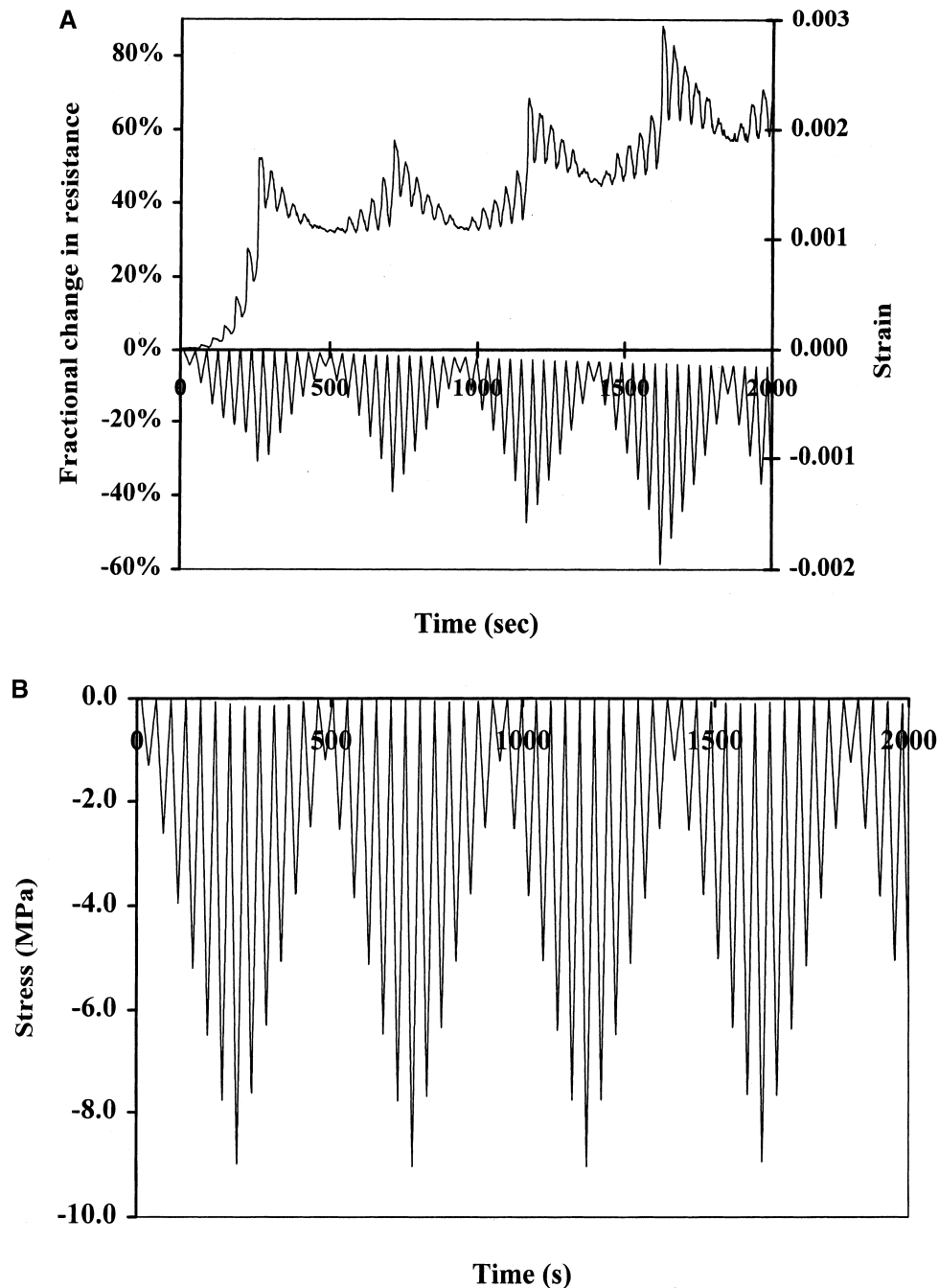


Fig. 5. Fractional change in resistance, strain (a) and stress (b) during repeated compressive loading at increasing and decreasing stress amplitudes, the highest of which was >90% of the compressive strength.

within a cycle, the resistance dropped and then increased sharply, reaching the maximum resistance of the extra peak at the maximum stress of the cycle. Upon subsequent unloading, the resistance decreased and then increased as unloading continued, reaching the maximum resistance of the original peak at zero stress. In the part of this group where the stress amplitude decreased cycle by cycle, the extra peak diminished and disappeared, leaving the original peak as the sole peak. In the part of the second group where the stress amplitude increased cycle by cycle, the original peak (peak at zero stress) was the sole peak, except that the extra peak (peak at the maximum stress) returned in a minor

way (more minor than in the first group) as the stress amplitude increased. The extra peak grew as the stress amplitude increased, but, in the part of the second group in which the stress amplitude decreased cycle by cycle, it quickly diminished and vanished, as in the first group. Within each group, the amplitude of resistance variation increased as the stress amplitude increased and decreased as the stress amplitude subsequently decreased. The baseline resistance decreased gradually from the first group to the second group.

Fig. 4 shows similar results for three successive groups with the highest stress amplitude being 60% of the com-

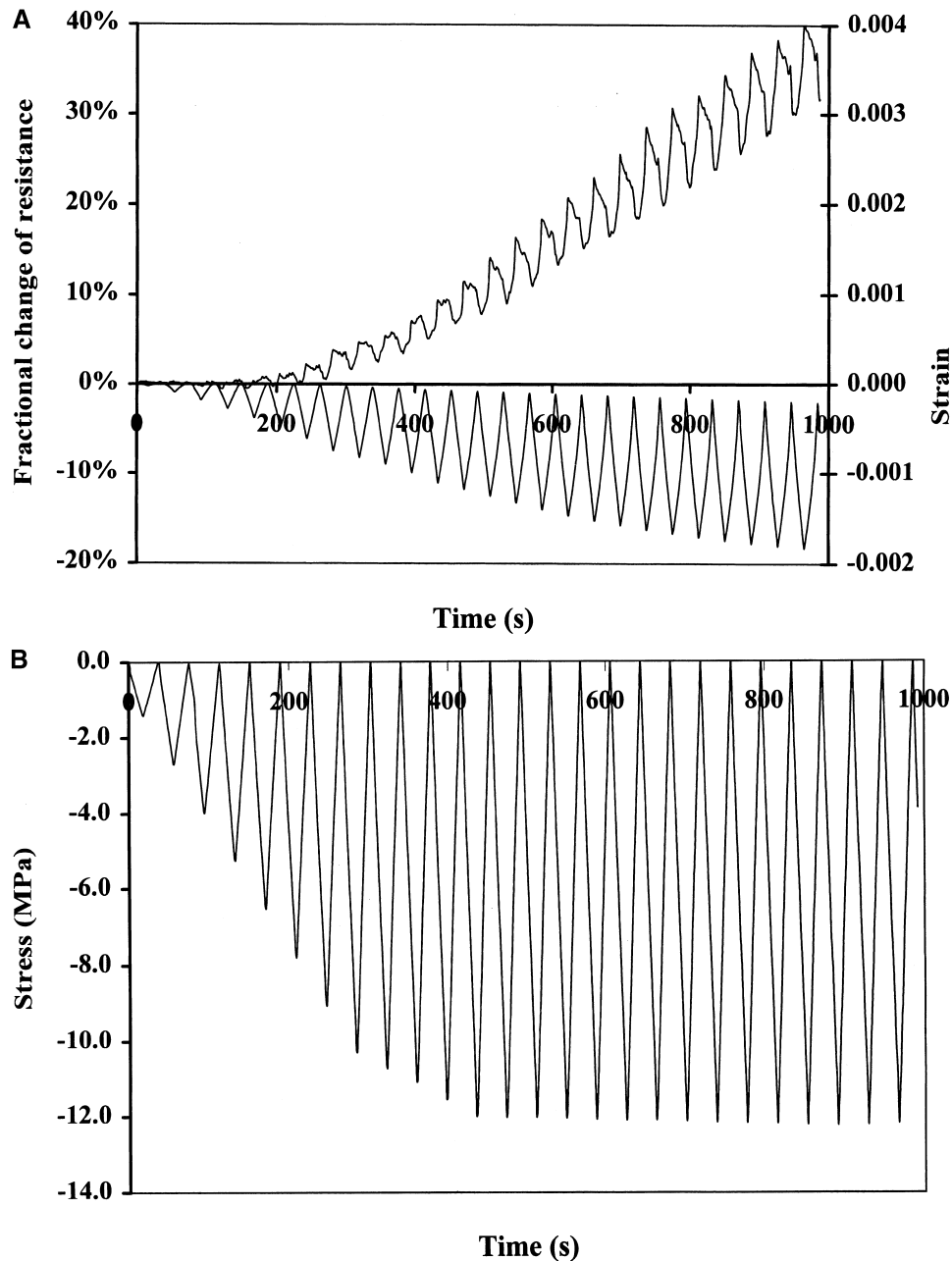


Fig. 6. Fractional change in resistance, strain (a) and stress (b) during repeated compressive loading at increasing stress amplitudes up to >90% of the compressive strength and then with the stress amplitude fixed at the maximum.

pressive strength. As the stress amplitude increased, the extra peak at the maximum stress of a cycle grew to the extent that it was comparable to the original peak at zero stress. The decrease of the baseline resistance from group to group was negligible, in contrast to Fig. 2. Other features of Figs. 2 and 4 are similar.

Fig. 5 shows four successive groups and the beginning of the fifth group, with the highest stress amplitude being more than 90% of the compressive strength. The highest stress amplitude was the same for each group (Fig. 5(b)), but the highest strain amplitude of a group increased from group to group as load cycling progressed (Fig. 5(a)). In contrast, the highest strain amplitude of a group did not change from group to group in Fig. 4(a). This means that the modulus decreased as cycling occurred in Fig. 5, whereas the modulus did not change in Fig. 4. In Fig. 5, the resistance increased in every cycle. The extra peak at the maximum stress of a cycle was the sole peak in each cycle. The original peak at zero stress did not appear at all. In each group, the amplitude of resistance change in a cycle increased with increasing stress amplitude and subsequently decreased with decreasing stress amplitude. In each group, the resistance increased abruptly as the maximum stress amplitude of the group was about to be reached. The baseline resistance increased gradually from group to group.

Fig. 6 shows the results for loading in which the stress amplitude increased cycle by cycle to a maximum (more than 90% of the compressive strength) and was held at the maximum for numerous cycles (Fig. 6(b)). The strain amplitude (Fig. 6(a)) increased along with the stress amplitude, but continued to increase after the stress amplitude had reached its maximum. This indicates a continuous decrease in modulus after the maximum stress amplitude had been reached. The resistance increased as the stress increased in each cycle, as in Fig. 5. The baseline resistance increased significantly cycle by cycle and continued to increase after the stress amplitude had reached its maximum.

4. Discussion

Carbon fiber-reinforced concrete is able to sense its own damage, which occurs under increasing stress even within the elastic regime. The damage is partially reversible, as indicated by the partially reversible increase in electrical resistivity observed during cyclic loading at a stress amplitude that increases cycle by cycle. In contrast, compressive strain is indicated by a reversible decrease in resistivity [5]. Upon increasing the stress, the resistance starts to increase at a stress higher than that in the prior cycles and continues to increase until the stress reaches the maximum in the cycle, thereby resulting in the extra peak at the maximum stress of a cycle in the part of a group in which the stress amplitude increases cycle by cycle. This resistance increase indicates the occurrence of damage. Upon decreasing the stress amplitude, the extra peak does not occur, except for the

first two cycles of stress amplitude decrease. The greater the stress amplitude, the larger and the less reversible is the damage-induced resistance increase (the extra peak). The partial irreversibility is clearly shown in Figs. 5 and 6. If the stress amplitude has been experienced before, the damage-induced resistance increase (the extra peak) is small, as shown by comparing the result of the second group with that of the first group (Figs. 2 and 4), unless the extent of damage is large (Figs. 5 and 6). When the damage is extensive (as shown by a modulus decrease), damage-induced resistance increase occurs in every cycle (Fig. 5), even at a fixed stress amplitude (Fig. 6) or at a decreasing stress amplitude (Fig. 5), and it can overshadow the strain-induced resistance decrease (Figs. 5 and 6). Hence, the damage-induced resistance increase occurs mainly during loading (even within the elastic regime), particularly at a stress above that in prior cycles, unless the stress amplitude is high and/or damage is extensive.

At a low-stress amplitude, the baseline resistance decreases irreversibly and gradually cycle by cycle (Figs. 1 and 2). This is the same as the effect reported in Ref. [6] and attributed to matrix damage and consequent enhancement of the chance of adjacent fibers to touch one another. At a high-stress amplitude, this baseline resistance decrease is overshadowed by the damage-induced resistance increase, the occurrence of which cycle by cycle as the stress amplitude increases causes the baseline resistance to increase irreversibly (Figs. 5 and 6). These two opposing baseline effects cause the baseline to remain flat at an intermediate stress amplitude (Fig. 4).

The baseline resistance in the regime of major damage (with a decrease in modulus) provides a measure of the extent of damage (i.e., condition monitoring). This measure works in the loaded or unloaded state. In contrast, the measure using the damage-induced resistance increase works only during stress increase and indicates the occurrence of damage (whether minor or major) as well as the extent of damage.

The damage causing the partially reversible damage-induced resistance increase is probably mainly associated with partially reversible degradation of the fiber–matrix interface. The reversibility rules out fiber fracture as the main type of damage, especially at a low-stress amplitude. At a high-stress amplitude, the extent of reversibility diminishes and fiber fracture may contribute to causing the damage. Fiber fracture can occur during the opening of a crack that is bridged by a fiber. The fiber–matrix interface degradation may be associated with slight fiber pull-out upon slight crack opening for cracks that are bridged by fibers. The severity of the damage-induced resistance increase supports the involvement of the fibers in the damage mechanism, as the fibers are much more conducting than the matrix.

In the regime of elastic deformation, the damage does not affect the strain permanently, as shown by the total reversibility of the strain during cyclic loading (Figs. 1–6).

Nevertheless, damage occurs during stress increase, as shown by the damage-induced resistance increase. Damage occurs even in the absence of a change in modulus. Hence, the damage-induced resistance increase is a sensitive indicator of minor damage (without a change in modulus), in addition to being a sensitive indicator of major damage (with a decrease in modulus). In contrast, the baseline resistance increase is an indicator of major damage only.

5. Conclusion

Damage in concrete reinforced with short carbon fibers was monitored by measurement of the DC electrical resistance in the stress direction during repeated compressive loading at increasing and decreasing stress amplitudes. Minor damage that was not accompanied by a change in compressive modulus was revealed by a partially reversible increase in resistance, which occurred mainly during loading, particularly at a stress above that in prior loading cycles. The greater the stress amplitude, the larger and the less reversible was the damage-induced resistance increase. Major damage that was accompanied by a decrease in modulus was revealed by the damage-induced resistance increase occurring in every loading cycle irrespective of the prior loading and by an irreversible increase in the baseline resistance. The damage-induced resistance increase was distinct from the strain-induced resistance decrease.

Acknowledgments

This work was supported by National Science Foundation, USA.

References

- [1] A.K. Pandey, M. Biswas, Damage detection in structures using changes in flexibility, *J Sound Vib* 169 (1) (1994) 3–17.
- [2] P. Chen, D.D.L. Chung, Concrete as a new strain/stress sensor, *Composites, Part B*, 27B (1996) 11–23.
- [3] P.-W. Chen, D.D.L. Chung, Low-drying-shrinkage concrete containing carbon fibers, *Composites, Part B*, 27B (1996) 269–274.
- [4] P.-W. Chen, D.D.L. Chung, A comparative study of concretes reinforced with carbon, polyethylene and steel fibers and their improvement by latex addition, *ACI Mater J* 93 (2) (1996) 129–133.
- [5] P.-W. Chen, D.D.L. Chung, Carbon fiber-reinforced concrete for smart structures capable of non-destructive flaw detection, *Smart Mater Struct* 2 (1993) 22–30.
- [6] X. Fu, D.D.L. Chung, Self-monitoring of fatigue damage in carbon fiber-reinforced cement, *Cem Concr Res* 26 (1) (1996) 15–20.
- [7] P.-W. Chen, X. Fu, D.D.L. Chung, Microstructural and mechanical effects of latex, methylcellulose and silica fume on carbon fiber-reinforced cement, *ACI Mater J* 94 (2) (1997) 147–155.
- [8] J. Hou, D.D.L. Chung, Cathodic protection of steel-reinforced concrete facilitated by using carbon fiber-reinforced mortar or concrete, *Cem Concr Res* 27 (5) (1997) 649–656.
- [9] X. Fu, E. Ma, D.D.L. Chung, W.A. Anderson, Self-monitoring in carbon fiber-reinforced mortar by reactance measurement, *Cem Concr Res* 27 (6) (1997) 845–852.
- [10] Z.-Q. Shi, D.D.L. Chung, Improving the abrasion resistance of mortar by adding latex and carbon fibers, *Cem Concr Res* 27 (8) (1997) 1149–1153.
- [11] N. Banthia, Carbon fiber cements: structure, performance, applications and research needs, in: J.I. Daniel, S.P. Shah (Eds.), *Fiber Reinf Concr*, ACI, SP-142, ACI, Detroit, MI, 1994, pp. 91–119.
- [12] H.A. Toutanji, T. El-Korchi, R.N. Katz, Strength and reliability of carbon-fiber-reinforced cement composites, *Cem Concr Compos* 16 (1994) 15–21.
- [13] P. Soroushian, M. Nagi, J. Hsu, Optimization of the use of lightweight aggregates in carbon fiber-reinforced cement, *ACI Mater J* 89 (3) (1992) 267–276.
- [14] H. Sakai, K. Takahashi, Y. Mitsui, T. Ando, M. Awata, T. Hoshijima, Flexural behavior of carbon fiber-reinforced cement composite, in: J.I. Shah, S.P. Shah (Eds.), *Fiber Reinf Concr*, ACI, SP-142, ACI, Detroit, MI, 1994, pp. 121–140.